Mitochondrial NADP$^+$-Dependent Isocitrate Dehydrogenase Deficiency Exacerbates Mitochondrial and Cell Damage after Kidney Ischemia-Reperfusion Injury

Sang Jun Han,* Hee-Seong Jang,* Mi Ra Noh,* Jinu Kim,† Min Jung Kong,* Jee In Kim,‡ Jeen-Woo Park,§ and Kwon Moo Park*

*Department of Anatomy, Cardiovascular Research Institute and Brain Korea 21 Plus, Kyungpook National University School of Medicine, Daegu, Republic of Korea; †Department of Anatomy, Jeju National University School of Medicine, Jeju-Do, Republic of Korea; ‡Department of Molecular Medicine and Medical Research Center, College of Medicine, Keimyung University, Daegu, Republic of Korea; and §Department of Biochemistry, School of Life Sciences and Biotechnology, College of Natural Sciences, Kyungpook National University, Daegu, Republic of Korea

ABSTRACT

Mitochondrial NADP$^+$-dependent isocitrate dehydrogenase (IDH2) catalyzes the oxidative decarboxylation of isocitrate to α-ketoglutarate, synthesizing NADPH, which is essential for mitochondrial redox balance. Ischemia-reperfusion (I/R) is one of most common causes of AKI. I/R disrupts the mitochondrial redox balance, resulting in oxidative damage to mitochondria and cells. Here, we investigated the role of IDH2 in I/R-induced AKI. I/R injury in mice led to the inactivation of IDH2 in kidney tubule cells. *Idh2* gene deletion exacerbated the I/R-induced increase in plasma creatinine and BUN levels and the histologic evidence of tubule injury, and augmented the reduction of NADPH levels and the increase in oxidative stress observed in the kidney after I/R. Furthermore, *Idh2* gene deletion exacerbated I/R-induced mitochondrial dysfunction and morphologic fragmentation, resulting in severe apoptosis in kidney tubule cells. In cultured mouse kidney proximal tubule cells, *Idh2* gene downregulation enhanced the mitochondrial damage and apoptosis induced by treatment with hydrogen peroxide. This study demonstrates that *Idh2* gene deletion exacerbates mitochondrial damage and tubular cell death *via* increased oxidative stress, suggesting that IDH2 is an important mitochondrial antioxidant enzyme that protects cells from I/R insult.

J Am Soc Nephrol 28: ●●●–●●●, 2016. doi: 10.1681/ASN.2016030349

Isocitrate dehydrogenases (IDHs) catalyze the oxidative decarboxylation of isocitrate to α-ketoglutarate, accompanied by the reduction of NAD(P)$^+$ to NAD(P)H.[1] Three IDHs, IDH1, IDH2, and IDH3, are present in mammals. IDH1 is localized in the cytosol, and IDH2 and IDH3 are localized in the mitochondria.[1] IDH3 is NAD$^+$-dependent, and it plays a central role in aerobic energy production in the tricarboxylic acid cycle.[1] IDH1 and IDH2 are NADP$^+$-dependent, and they have important roles in cellular metabolism. IDH1 is involved in lipid metabolism and glucose sensing, and IDH2 is involved in the regulation of oxidative respiration.[1] Accumulating evidence consistently demonstrates that NADPH levels generated by IDH1 and IDH2 are critical for the maintenance of redox balance *via* the glutathione and thioredoxin systems of peroxide detoxification.[1–4] NADPH is necessary for the antioxidative action of both the

Received March 25, 2016. Accepted September 26, 2016.

Published online ahead of print. Publication date available at www.jasn.org.

Correspondence: Prof. Kwon Moo Park, Department of Anatomy, Kyungpook National University School of Medicine, 101 Dongindong, Junggu, Daegu 700-422, Republic of Korea, or Prof. Jeen-Woo Park, School of Life Sciences and Biotechnology, College of Natural Sciences, Kyungpook National University, Taegu 702-701, Republic of Korea. E-mail: kmpark@knu.ac.kr or parkjw@knu.ac.kr

Copyright © 2016 by the American Society of Nephrology

thioredoxin and glutathione systems.[1,5] The intracellular concentration of thioredoxin is 100–1000-fold lower than that of glutathione.[5] Recent studies have reported that IDH2 is a major NADPH-producing enzyme, and that IDH2 is important for maintaining the mitochondrial redox balance in cells.[6–9] However, the role of IDH2 in kidney diseases remains to be defined.

AKI is common in patients within intensive care units. AKI is associated with high mortality and morbidity, and is a risk factor for developing CKD. Ischemia-reperfusion (I/R) injury is the most common cause of AKI. Increasing evidence demonstrates that reactive oxygen species (ROS) and oxidative stress play a crucial role in the pathogenesis of I/R-induced AKI.[10] Mitochondria are the major producers of ROS in the cell. Simultaneously, mitochondria comprise one of the intracellular organelles most susceptible to ROS.[11,12] Mitochondria produce most of the energy used by the cell *via* oxidative phosphorylation. Oxidative phosphorylation is the major endogenous source of ROS, such as the superoxide anion radical (O_2^-), hydrogen peroxide (H_2O_2), and the hydroxyl radical, all of which are toxic byproducts. Under physiologic conditions, ROS are tightly regulated within the mitochondria by various mechanisms, including the actions of mitochondrial manganese superoxide dismutase (MnSOD) and glutathione peroxidase (GPx). MnSOD converts O_2^- to H_2O_2, and GPx converts H_2O_2 to H_2O in the presence of GSH.[13] However, under pathophysiologic conditions, such as when the ROS production and removal systems are broken, excessive amounts of ROS are generated, resulting in acute/chronic exposure of mitochondria to ROS. ROS stress in the mitochondria leads to the shutdown of mitochondrial energy production, and causes oxidative damage to mitochondrial and cellular proteins, lipids, and nucleic acids.[14] Many studies have demonstrated that maintenance of the mitochondrial redox balance, by genetic or pharmacologic approaches, protects cells against AKI.[11,15,16]

During I/R injury, superoxide radicals (ROS produced primarily in the mitochondria) are rapidly converted to H_2O_2 by MnSOD. The noxious H_2O_2 is removed by GPx and other members of the peroxiredoxin family.[13] GPx requires GSH in order to remove H_2O_2. NADPH is required for the reduction of oxidized glutathione (GSSG) by glutathione reductase (GR).[17] GSH is also needed to detoxify lipid peroxides through the action of glutathione-S-transferases. Therefore, NADPH is an essential cofactor for the removal of noxious oxygen free radicals produced by I/R. It is classically recognized that glucose 6-phosphate dehydrogenase (G6PD), which catalyzes the first reaction in the pentose phosphate pathway, is as a major NADPH-producing enzyme.[13] However, G6PD is absent from mitochondria, and the inner membrane of mitochondria is impermeable to NADPH.[1,18] Therefore, we hypothesized that IDH2, by providing mitochondrial NADPH, is important for the prevention of I/R-induced mitochondrial damage and consequent AKI. We report here, for the first time, that *Idh2* gene deletion exacerbates I/R-induced mitochondrial damage, oxidative stress, apoptosis, and necrosis, and we suggest that IDH2 is a useful target to develop therapeutics for AKI.

RESULTS

Idh2 Gene Deficiency Exacerbates Kidney Injury after I/R Insult

The survival rate after ischemia was much lower in $Idh2^{-/-}$ mice than in $Idh2^{+/+}$ mice (Figure 1A). BUN and plasma creatinine (PCr) concentrations increased in both $Idh2^{+/+}$ and $Idh2^{-/-}$ mice after ischemia (Figure 1, B and C). The increases in BUN and PCr concentrations were greater in $Idh2^{-/-}$ mice than in $Idh2^{+/+}$ mice (Figure 1, B and C). As previously described,[19] BUN concentrations peaked at 1 day after ischemia, and then decreased gradually to near-normal levels (Figure 1B, note that BUN was determined only in mice that survived), indicating that the functional recovery of the kidney was delayed in $Idh2^{-/-}$ mice compared with $Idh2^{+/+}$ mice (Figure 1B). Consistent with the results for functional damage, I/R resulted in severe damage to kidneys of both $Idh2^{+/+}$ and $Idh2^{-/-}$ mice; post-I/R kidneys presented with congestion and dilation of tubules, loss of brush border and nuclei in tubular cells, and accumulation of interstitial cells (Figure 1, D–F). The damage was greater in $Idh2^{-/-}$ mice than in $Idh2^{+/+}$ mice (Figure 1, D–F). Sixteen days after ischemia, the expression of collagen increased in the interstitium, and this increase was greater in $Idh2^{-/-}$ mice than in $Idh2^{+/+}$ mice (Figure 1, G and H), indicating that kidney injury is more severe in $Idh2^{-/-}$ mice than in $Idh2^{+/+}$ mice. F4/80 is a marker of monocyte/macrophage cells. F4/80-positive cells were observed mainly in the interstitium at 1 day and 16 days after ischemia (Figure 1I). The number of F4/80-positive cells was greater in $Idh2^{-/-}$ mice than in $Idh2^{+/+}$ mice (Figure 1, I–K). The expression of Ly6G, a neutrophil marker, increased in both $Idh2^{+/+}$ and $Idh2^{-/-}$ mice 24 hours after ischemia (Figure 1, L and M). This increase was greater in $Idh2^{-/-}$ mice than in $Idh2^{+/+}$ mice (Figure 1, L and M). There were no significantly differences in PCr and BUN concentrations, histologic damage, F4/80-positive cell number, Ly6G expression, and collagen expression in sham-operated $Idh2^{-/-}$ mice when compared with $Idh2^{+/+}$ mice (Figure 1). Taken together, these data indicate that *Idh2* gene deletion exacerbates kidney injury after I/R insult.

I/R Reduces IDH2 Expression and Activity in Both $Idh2^{+/+}$ and $Idh2^{-/-}$ Kidneys

IDH2 was observed throughout the entirety of the tubules in wild-type mouse kidneys. The most intense IDH2 expression was seen in the collecting duct, proximal tubule, distal tubule, and descending thin limb, in that order (Figure 2, A and B). Twenty-four hours after ischemia, IDH2 expression decreased in all tubules, and those decreases were greatest in the proximal tubule and distal tubule (Figure 2A). Further, when IDH2 expression was evaluated in the kidneys by Western blot analysis, expression was lower from 1 day to 16 days after ischemia (Figure 2C). IDH1 expression decreased 1 day after ischemia and then returned to around normal level by 16 days after ischemia (Figure 2C).

When we determined IDH1 and IDH2 expression and activity in the $Idh2^{+/+}$ and $Idh2^{-/-}$ mouse kidneys, expression of

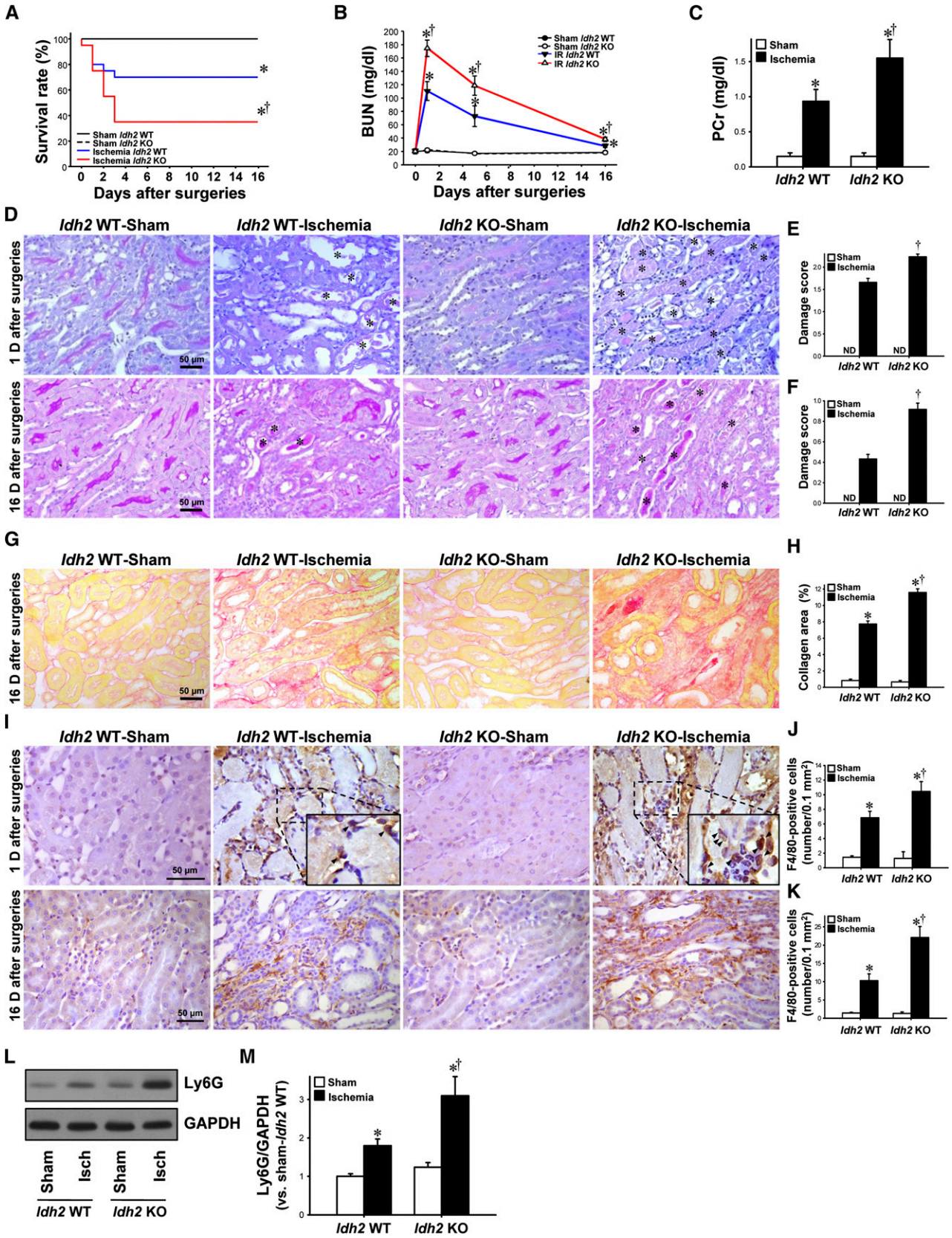

Figure 1. Renal function, histology, and inflammation in *Idh2*$^{+/+}$ and *Idh2* $^{-/-}$ mice after I/R. *Idh2*$^{+/+}$ (*Idh2* WT) and *Idh2*$^{-/-}$ (*Idh2* KO) mice were subjected to either 25 minutes of bilateral renal ischemia or a sham surgery. (A) Survival rate was determined (each group *n*=20). (B) Concentrations

both IDH2 and IDH1 had decreased in *Idh2*$^{+/+}$ mice 24 hours after ischemia. IDH2 was not detected in *Idh2*$^{-/-}$ mice (Figure 2, D and E). IDH1 expression decreased in both *Idh2*$^{+/+}$ and *Idh2*$^{-/-}$ mice after I/R, and this decrease was greater in *Idh2*$^{-/-}$ mice (Figure 2, D and F). When the level of activity of IDH2 and IDH1 was determined in the mitochondrial and cytosolic fractions of the kidney (Figure 2G), it was established that I/R had decreased the activity of both IDH2 and IDH1 in *Idh2*$^{+/+}$ mice (Figure 2, H and I). IDH2 activity was not detected in *Idh2*$^{-/-}$ mice (Figure 2H). IDH3 activity decreased in both *Idh2*$^{+/+}$ and *Idh2*$^{-/-}$ mice after I/R, but there was no significant difference in post-I/R IDH3 activity between *Idh2*$^{-/-}$ and *Idh2*$^{+/+}$ mice (Figure 2J). IDH3 activity was not significantly different between *Idh2*$^{+/+}$ mice and *Idh2*$^{-/-}$ mice after sham operation (Figure 2J). IDH1 activity decreased in both *Idh2*$^{+/+}$ and *Idh2*$^{-/-}$ mice after I/R, and this decrease was greatest in *Idh2*$^{-/-}$ mice (Figure 2I). Interestingly, IDH1 expression and activity in sham-operated *Idh2*$^{-/-}$ mice was slightly lower than in sham-operated *Idh2*$^{+/+}$ mice (Figure 2, D, F, and I). These results indicate that I/R insult disrupts the functioning of IDHs.

Idh2 Gene Deletion Exacerbates ROS Production and Oxidative Stress after I/R

To investigate whether the increased susceptibility of kidneys to I/R insult in *Idh2*$^{-/-}$ mice is associated with ROS/oxidative stress, we measured ROS production and oxidative stress levels in the kidneys 24 hours after ischemia. Twenty-four hours after ischemia, the H_2O_2 level was greater in *Idh2*$^{-/-}$ mice than in *Idh2*$^{+/+}$ mice (Figure 3A). MDA production and 4-hydroxynonenal (4-HNE) expression, indexes of lipid peroxidation, increased in both *Idh2*$^{+/+}$ and *Idh2*$^{-/-}$ mice 24 hours after ischemia (Figure 3, B–D). These post-I/R increases in MDA production and 4-HNE expression were greater in *Idh2*$^{-/-}$ mice than in *Idh2*$^{+/+}$ mice (Figure 3, B–D). The H_2O_2 level, MDA amount, and expression of 4-HNE were slightly greater in the sham-operated *Idh2*$^{-/-}$ mice than *Idh2*$^{+/+}$ mice (Figure 3, A–D). When oxidative damage to DNA was evaluated by immunostaining using an anti–8-hydroxy-2′-deoxyguanosine (8-OHdG) antibody,[20] 8-OHdG–positive signals were observed in both the cytosol and nuclei of tubule cells, in both *Idh2*$^{+/+}$ and *Idh2*$^{-/-}$ mice 24 hours after ischemia (Figure 3E), indicating that mitochondrial and nuclear DNA are oxidatively damaged. The number of 8-OHdG–positive cells and the intensity of 8-OHdG staining in the cytosol were greater in *Idh2*$^{-/-}$ mice than in *Idh2*$^{+/+}$ mice (Figure 3, E–G). These results indicate that *Idh2* gene deletion exacerbates oxidative stress after I/R.

Idh2 Gene Deletion Impairs Reduction of $NADP^+$ and GSSG within Mitochondria after I/R

When NADPH levels were evaluated by immunohistochemical staining using an anti-NADPH antibody, NADPH was found to have decreased in kidney tubular cells 24 hours after ischemia (Figure 4A). This decrease in NADPH was greater in *Idh2*$^{-/-}$ mice than in *Idh2*$^{+/+}$ mice (Figure 4A). After a sham operation, NADPH was lower in *Idh2*$^{-/-}$ mice than in *Idh2*$^{+/+}$ mice (Figure 4A).

The activity of mitochondrial GR decreased in both *Idh2*$^{-/-}$ and *Idh2*$^{+/+}$ mice 24 hours after ischemia (Figure 4B). This decrease in GR activity was greater in *Idh2*$^{-/-}$ mice than in *Idh2*$^{+/+}$ mice (Figure 4B). However, there was no significant difference in GR activity between *Idh2*$^{-/-}$ and *Idh2*$^{+/+}$ mice after sham operation (Figure 4B). The ratio of GSSG to total glutathione (GSSG/tGSH) in the mitochondria increased 24 hours after ischemia in both *Idh2*$^{-/-}$ and *Idh2*$^{+/+}$ mice (Figure 4C). This ratio was significantly more increased in *Idh2*$^{-/-}$ mice than in *Idh2*$^{+/+}$ mice (Figure 4C). However, there was no significant difference in the GSSG/tGSH ratio between sham-operated *Idh2*$^{-/-}$ mice and *Idh2*$^{+/+}$ mice (Figure 4C). These data indicate that, upon I/R injury, *Idh2* gene deletion impairs the process whereby GSSG is reduced to GSH within mitochondria. GPx uses GSH to remove H_2O_2 in mitochondria.[21] Twenty-four hours after ischemia, mitochondrial GPx activity had decreased in both *Idh2*$^{-/-}$ and *Idh2*$^{+/+}$ mice (Figure 4D). This decrease in GPx activity was greater in *Idh2*$^{-/-}$ mice than in *Idh2*$^{+/+}$ mice (Figure 4D). However, there was no significant difference in GPx activity between *Idh2*$^{-/-}$ and *Idh2*$^{+/+}$ mice after a sham operation (Figure 4D). These results indicate that a decline in NADPH production owing to *Idh2* gene deletion may impair GPx-mediated removal of H_2O_2 in mitochondria.

Further, we determined whether IDH2 affects the GSSG/tGSH ratio, or the activity of GR and GPx, in the cytosolic fraction of kidney lysates. The activity of cytosolic GR decreased 24 hours after ischemia in both *Idh2*$^{+/+}$ and *Idh2*$^{-/-}$ mice (Figure 5A). The GSSG/tGSH ratio increased in both *Idh2*$^{+/+}$ and *Idh2*$^{-/-}$ mice (Figure 5B). The activity of cytosolic GPx decreased 24 hours after ischemia in both *Idh2*$^{+/+}$ and *Idh2*$^{-/-}$ mice (Figure 5C).

of BUN were measured at indicated times. (C) Concentrations of PCr were determined 24 hours after surgery. (D) Twenty-four hours (upper panels) and 16 days (lower panels) after surgery, kidneys were harvested and then stained with periodic acid–Schiff. Images were obtained from the outer medulla. Asterisk indicates congestion of necrotic tubule cells. (E and F) Kidney damage was scored as described in the Concise Methods section. (G) Sixteen days after surgery, kidney sections were subjected to picro-sirius red staining. (H) Collagen deposition was measured as described in the Concise Methods section. (I) Twenty-four hours (upper panels) and 16 days (lower panels) after surgery, kidney sections were subjected to immunohistochemical staining using an anti-F4/80 antibody. Hematoxylin was used to visualize the nuclei of cells. Insert is at high magnification of the dash-lined rectangle. Arrows indicate F4/80-positive cells. (J and K) F4/80-positive cells were counted in the outer stripe of outer medulla. (L) Twenty-four hours after surgery, kidney samples were analyzed by Western blotting using an anti-Ly6G antibody. GAPDH was used as a loading control. (M) The density of band was measured using ImageJ software. Results are expressed as mean±SEM (n=6 except survival rate). *$P<0.05$ versus respective sham-operated mice; †$P<0.05$ versus ischemia-operated *Idh2* WT mice. Isch, ischemia; KO, knockout; ND, not detected; WT, wild type.

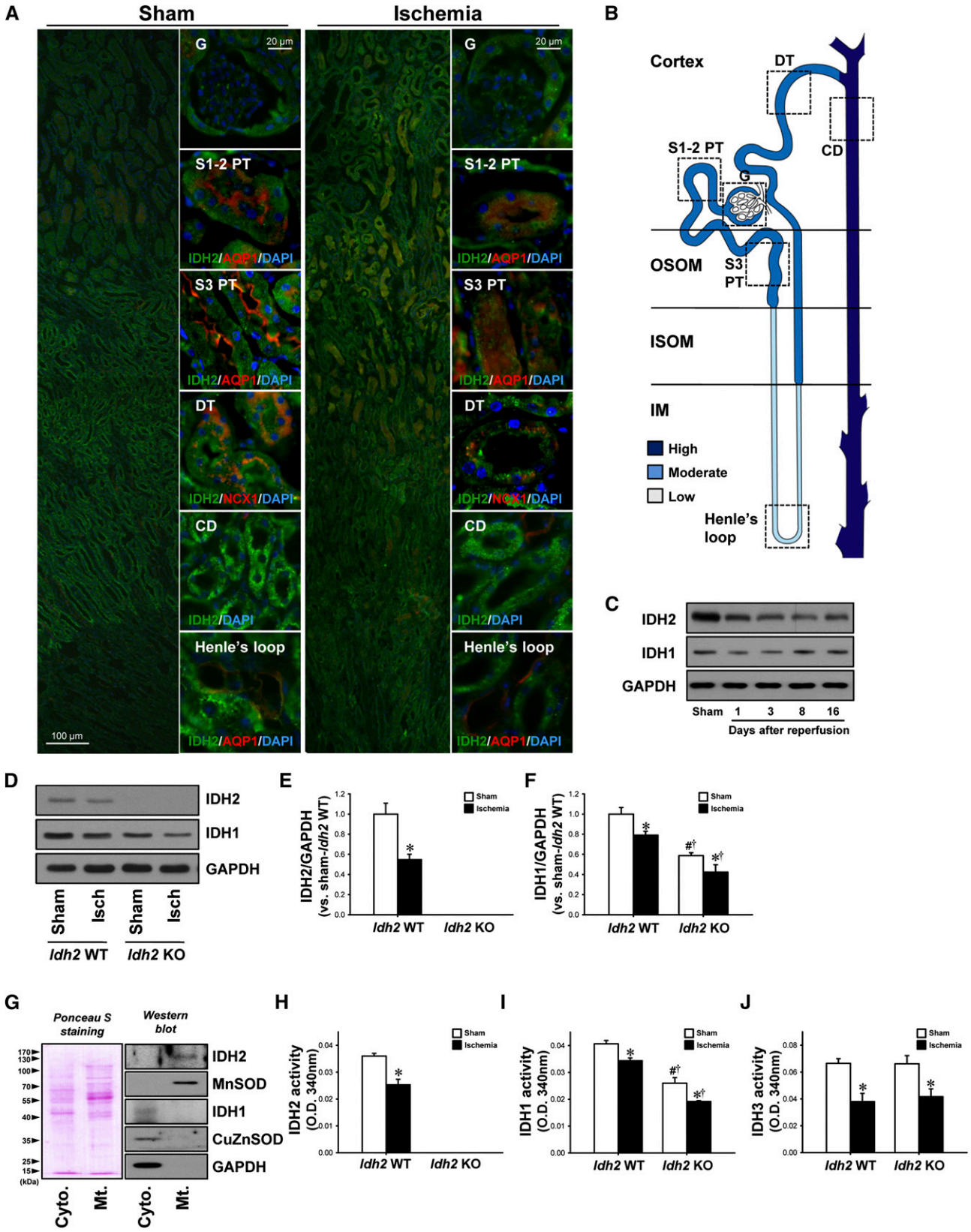

Figure 2. Expression and activity of IDH2 and IDH1 in *Idh2*$^{+/+}$ and *Idh2*$^{-/-}$ mice after I/R. C57BL/6 mice were subjected to either renal ischemia or a sham operation. (A) Twenty-four hours after surgery, kidney sections were subjected to immunofluorescence staining using antibodies directed against IDH2, AQP1, and NCX1. 4′,6-diamidino-2-phenylindole (DAPI) staining was used to visualize the nuclei of

However, there were no significant differences between *Idh2*$^{+/+}$ and *Idh2*$^{-/-}$ mice in the activity of GPx or GR, or in GSSG/tGSH (Figure 5, A–C). This indicates that IDH2 is not critical for the activity of cytosolic GR or GPx. Because it has been classically recognized that G6PD is a major producer of NADPH and catalase is a major H_2O_2–removing enzyme in the cytosol, we determined the activities and expressions of G6PD and catalase in the cytosol. The expressions and activities of G6PD and catalase decreased after I/R in both *Idh2*$^{-/-}$ and *Idh2*$^{+/+}$ mice (Figure 5, D–H). However, there were no significant differences in the expression or activity of G6PD or catalase between *Idh2*$^{+/+}$ and *Idh2*$^{-/-}$ mice (Figure 5, D–H). Taken together, these data indicate that IDH2 is a critical enzyme for the GSH–peroxide detoxification system in mitochondria.

Idh2 Gene Deletion Exacerbates Structural and Functional Damage to Mitochondria after I/R

ROS and oxidative stress causes structural and functional damage to mitochondria, including fragmentation.[12] Transmission electron microscopy data revealed swelling of mitochondria with a loss of cristae, disruption of the mitochondrial membrane, and release of matrix content into the cytoplasm 90 minutes post-ischemia (Figure 6A). These examples of post-I/R mitochondrial damage were more severe in *Idh2*$^{-/-}$ mice than in *Idh2*$^{+/+}$ mice (Figure 6A). The ATP level was significantly lower in *Idh2*$^{-/-}$ kidneys than in *Idh2*$^{+/+}$ kidneys, at 24 hours after ischemia (Figure 6B). There was no significant difference in the ATP level between sham-operated *Idh2*$^{+/+}$ mice and *Idh2*$^{-/-}$ mice (Figure 6B). To evaluate mitochondrial fragmentation, we determined the mitochondrial aspect ratio (the ratio between the major and minor axis of the ellipse equivalent to the mitochondrion). After ischemia, the mitochondrial aspect ratios decreased in both *Idh2*$^{-/-}$ and *Idh2*$^{+/+}$ mice, although the decrease seen in *Idh2*$^{+/+}$ mice was not statistically significant (Figure 6C). The mitochondrial aspect ratio recorded in sham-operated *Idh2*$^{-/-}$ mice was lower than that in *Idh2*$^{+/+}$ mice (Figure 6C).

The expression of dynamin-related protein 1 (Drp1) and fission 1 protein (Fis1), markers of mitochondrial fission, was increased in the kidneys of both *Idh2*$^{+/+}$ and *Idh2*$^{-/-}$ mice (Figure 6, D–F). These increases in Drp1 and Fis1 expression were greater in *Idh2*$^{-/-}$ mice than in *Idh2*$^{+/+}$ mice (Figure 6, D–F). The expression of both Drp1 and Fis1 was higher in sham-operated *Idh2*$^{-/-}$ mice than in sham-operated *Idh2*$^{+/+}$ mice (Figure 6, D–F). In contrast to the fission proteins, the expression of optic atrophy 1 (Opa1), a marker of mitochondrial fusion, was decreased in *Idh2*$^{-/-}$ mice, but not in *Idh2*$^{+/+}$ mice, 24 hours after ischemia (Figure 6, D and G). There was no significant difference in the expression of Opa1 between sham-operated *Idh2*$^{+/+}$ mice and *Idh2*$^{-/-}$ mice. This indicates that *Idh2* gene deletion impairs the balance between mitochondrial fusion and fission, resulting in increased fragmentation. It also suggests that IDH2 plays a crucial role in the maintenance of mitochondrial structure and function, and that its disruption increases the vulnerability of mitochondria to I/R insults.

Idh2 Gene Deletion Exacerbates Apoptosis of Tubular Cells after I/R

Mitochondrial damage initiates the apoptotic cascade.[12] First, we determined the expression of Bax and Bcl family proteins, which regulate cytochrome *c* release from the mitochondria into the cytosol. After I/R, the expression of proapoptotic factor Bax (active [6A7] and total [5B7] form of Bax) increased in both *Idh2*$^{+/+}$ and *Idh2*$^{-/-}$ mice (Figure 7, A–C). In contrast, the expressions of antiapoptotic factors, Bcl-2 and Bcl-xL, were decreased in both *Idh2*$^{+/+}$ and *Idh2*$^{-/-}$ mice (Figure 7, A, D, and F). The ratio of total Bax-to-Bcl-2 increased in both *Idh2*$^{+/+}$ and *Idh2*$^{-/-}$ mice (Figure 7E). Those post-I/R changes in proapoptotic and antiapoptotic factors were greater in *Idh2*$^{-/-}$ mice than *Idh2*$^{+/+}$ mice (Figure 7, A–H). Next, to evaluate cytochrome *c* release, we determined the expression of cytochrome *c* in the mitochondria and the cytosol, respectively. I/R decreased the level of mitochondrial cytochrome *c* expression when compared with sham, whereas I/R increased the level of cytosolic cytochrome *c* expression (Figure 7, I–K). These post-I/R changes were greater in in *Idh2*$^{-/-}$ mice than *Idh2*$^{+/+}$ mice (Figure 7, I–K). These results indicate that I/R in *Idh2*$^{-/-}$ mice induces greater mitochondrial damage than in *Idh2*$^{+/+}$ mice. Further, we determined levels of expression of caspase-3 and X-linked inhibitor-of-apoptosis protein (XIAP), an antiapoptotic protein. I/R increased caspase-3 expression, whereas it decreased XIAP expression in both *Idh2*$^{+/+}$ and *Idh2*$^{-/-}$ mice (Figure 7, A, G, and H). These changes were greater in *Idh2*$^{-/-}$ mice than in *Idh2*$^{+/+}$ mice (Figure 7, A, G, and H).

I/R injury significantly increased terminal deoxynucleotidyl transferase–mediated digoxigenin-deoxyuridine nick-end labeling

cells. (B) Diagram showing IDH2 expression in normal kidney tubular segments. (C) Kidneys were harvested at the indicated times and analyzed by Western blotting using anti-IDH2 and anti-IDH1 antibodies. GAPDH was used as a loading control. (D) *Idh2*$^{+/+}$ and *Idh2*$^{-/-}$ mice were subjected to 25 minutes of renal ischemia. Kidneys were harvested 24 hours after ischemia and then subjected analyzed by Western blotting using anti-IDH2 and anti-IDH1 antibodies. (E and F) The densities of bands were measured using ImageJ software. (G) The mitochondria and cytosol mitochondria were fractionated from kidney whole lysates, and the fractions were then confirmed by Western blot analysis using antibodies directed against IDH2, MnSOD, IDH1, CuZnSOD, and GAPDH. Ponceau S was used to determine equal loading. The activity of IDH2 (H), IDH1 (I), and IDH3 (J) was measured in the mitochondrial (H and J) and cytosolic fractions (I), respectively. Results are expressed as the mean±SEM (n=6). *P<0.05 versus respective sham-operated mice; †P<0.05 versus ischemia-operated *Idh2* WT mice; #P<0.05 versus sham-operated *Idh2* WT mice. CD, collecting duct; DT, distal tubule; G, glomerulus; Isch, ischemia; ISOM, inner stripe of outer medulla; KO, knockout; OSOM, outer stripe of outer medulla; S1–2 PT, segment 1–2 in the proximal tubule; S3 PT, segment 3 in proximal tubule; WT, wild type.

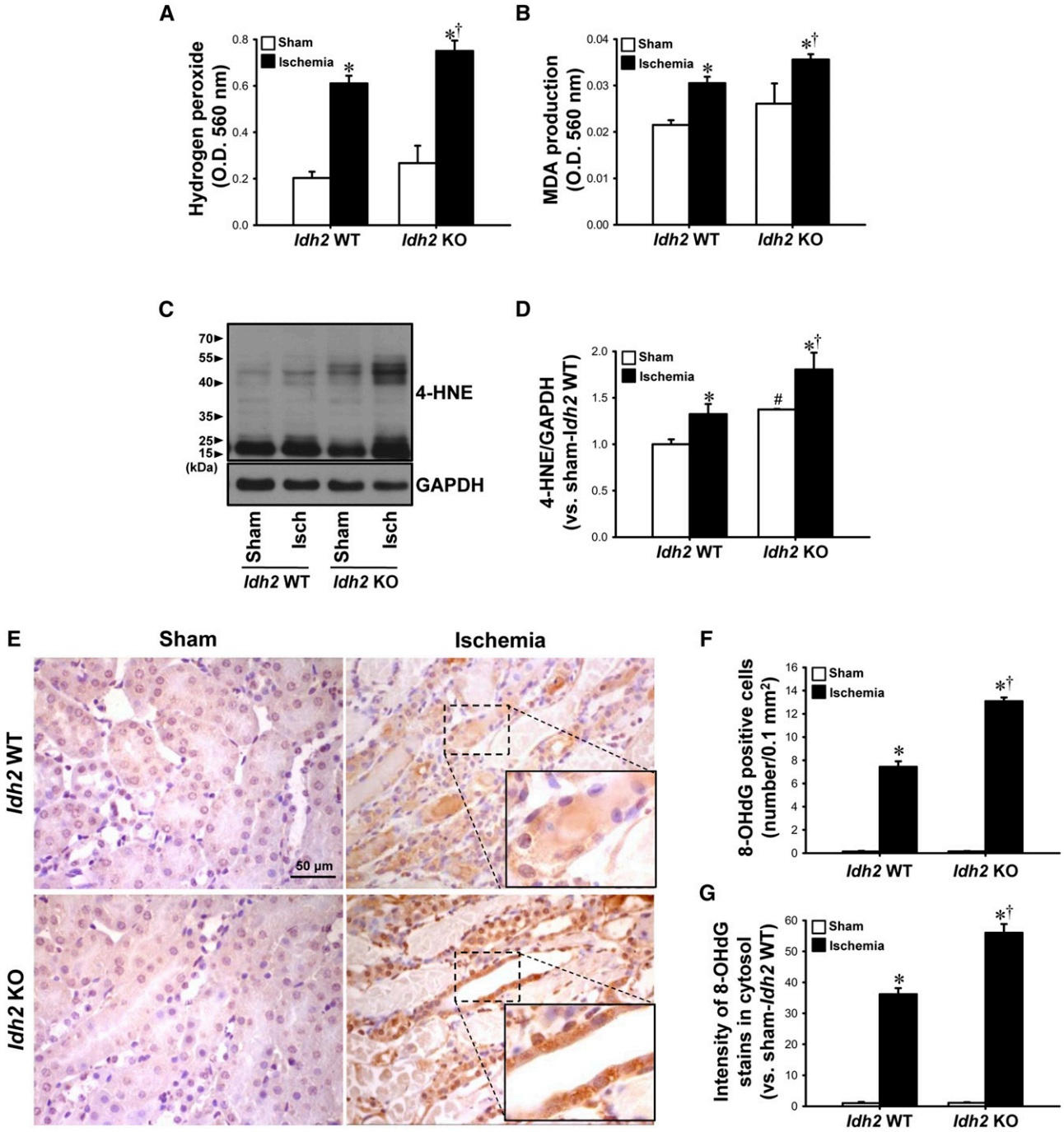

Figure 3. *Idh2* gene deletion accelerates H_2O_2 production, lipid peroxidation, and DNA oxidation in the kidneys after I/R. *Idh2*$^{+/+}$ (*Idh2* WT) and *Idh2*$^{-/-}$ (*Idh2* KO) mice were subjected to either 25 minutes of bilateral renal ischemia or sham surgery, and then kidneys were harvested 24 hours later. H_2O_2 (A) and MDA production (B) were determined in the kidney tissue. (C) 4-HNE expression was determined by Western blot analysis using an anti–4-HNE antibody. GAPDH was used as a loading control. (D) The densities of bands were measured using ImageJ software. (E) Kidney sections were subjected to immunohistochemical staining using an 8-OHdG antibody. Images were obtained from the outer medulla. Insert is at high magnification of the dash-lined rectangles. Brown indicates 8-OHdG-positive signal. Number of 8-OHdG–positive cells (F) and intensity of the 8-OHdG stains in the cytosol (G) were determined. Results are expressed as mean±SEM (n=6). *P<0.05 versus respective sham-operated mice; †P<0.05 versus ischemia-operated *Idh2* WT mice; #P<0.05 versus sham-operated *Idh2* WT mice. Isch, ischemia; KO, knockout; WT, wild type.

(TUNEL)-positive tubule cells in both *Idh2*$^{+/+}$ and *Idh2*$^{-/-}$ mice 24 hours after ischemia, and these increases in TUNEL-positive cells were greater in *Idh2*$^{-/-}$ mice than in *Idh2*$^{+/+}$ mice (Figure 7, L and M). Sixteen days after ischemia, the amount of TUNEL-positive cells was greater in the kidneys of *Idh2*$^{-/-}$ mice than in *Idh2*$^{+/+}$ mice (Figure 7, L and N). In sham-operated kidneys, the

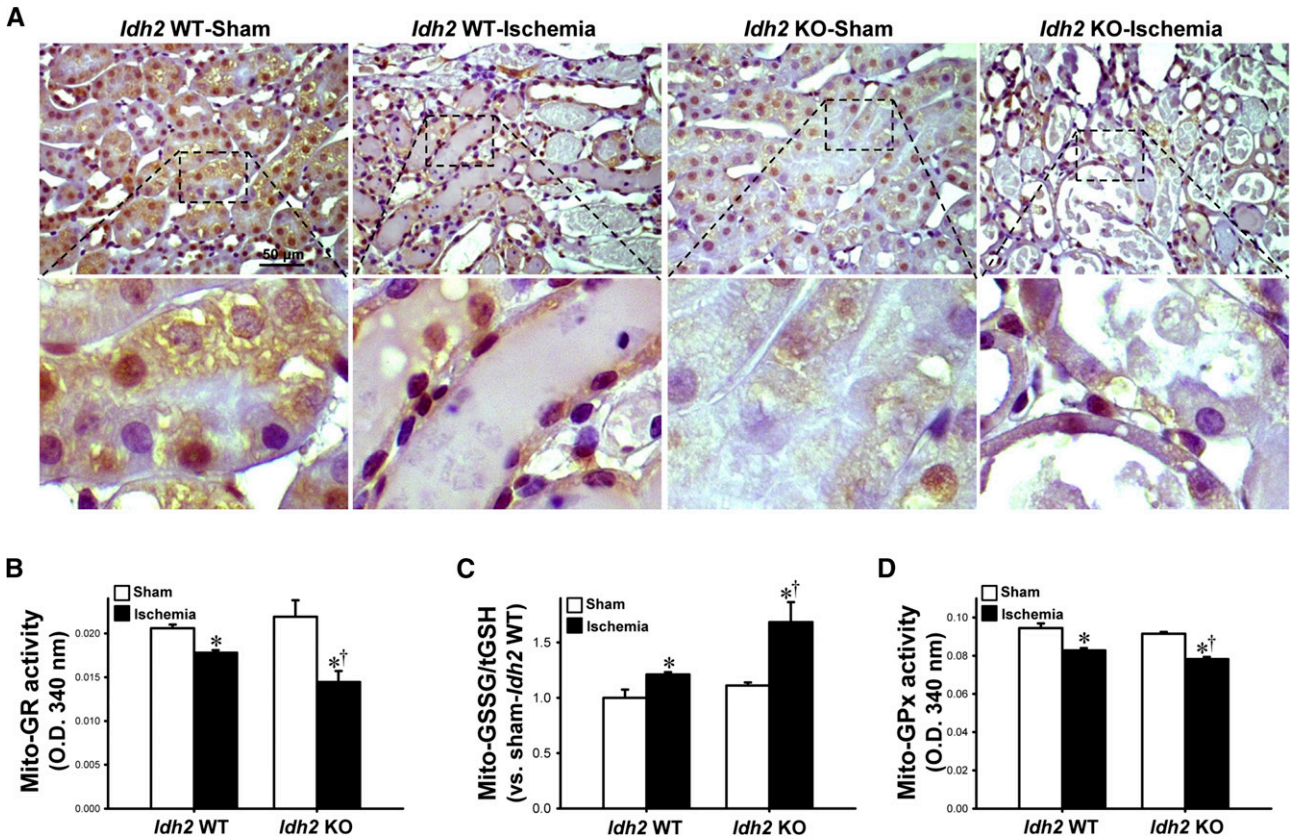

Figure 4. Levels of NADPH, activity of GR and GPx, and GSSG/tGSH in the mitochondria from *Idh2*$^{+/+}$ and *Idh2*$^{-/-}$ mice after I/R. *Idh2*$^{+/+}$ (*Idh2* WT) and *Idh2*$^{-/-}$ (*Idh2* KO) mice were subjected to either 25 minutes of bilateral renal ischemia or sham surgery. (A) Kidney sections were subjected to immunohistochemical staining using an anti-NAPDH antibody. Images were obtained from the outer medulla. Upper panels are at low magnification, lower panels are at high magnification of the dash-lined rectangle in upper panel. Brown indicates NADPH-positive signal. (B) Activity of GR, (C) GSSG/tGSH, and (D) the activity of GPx in the mitochondrial fractions from kidneys were determined as described in the Concise Methods section. Results are expressed as the mean±SEM (n=6). *P<0.05 versus respective sham-operated mice; †P<0.05 versus ischemia-operated *Idh2* WT. KO, knockout; WT, wild type.

expression of Bax (5B7), Bcl-2, and Bcl-xL was greater in *Idh2*$^{-/-}$ mice than in *Idh2*$^{+/+}$ mice (Figure 7, A–H). However, there were no significant differences in TUNEL-positive cells, active form of Bax (Bax 6A7), and caspase-3 activation between sham-operated *Idh2*$^{-/-}$ mice and *Idh2*$^{+/+}$ mice (Figure 7). These data indicate that *Idh2* gene deletion accelerates the apoptosis pathway and delays recovery after I/R insult.

Idh2 Gene Downregulation Exacerbates H_2O_2-Induced Apoptosis in Cultured Proximal Tubule Cells

Finally, we determined whether IDH2 downregulation, using small interfering RNA (siRNA) against *Idh2* (*Idh2*-siRNA), increases the susceptibility of murine proximal tubular epithelial cells (mProx24 cells) to H_2O_2-induced oxidative stress and ATP depletion/repletion. First, we determined the role of IDH2 on H_2O_2-induced oxidative stress. *Idh2*-siRNA transfection significantly decreased IDH2 expression in the cells (Figure 8, A and B). H_2O_2 treatment decreased expression of IDH2 in both *Idh2*-siRNA–transfected cells and scramble-siRNA–transfected cells (Figure 8, A and B). The decrease was greater in *Idh2*-siRNA–transfected cells than in scramble-siRNA–transfected cells (Figure 8, A and B). H_2O_2 treatment increased the expression of Bax (6A7), the ratio of Bax (5B7) to Bcl-2 expression, and cleaved caspase-3. These increases were higher in the *Idh2*-siRNA–transfected cells (Figure 8, A, C, D, and H). In contrast, H_2O_2 treatment lowered the expression of Bcl-2, Bcl-xL, and XIAP, and the decreases were greater in *Idh2*-siRNA–transfected cells (Figure 8, A, E, F, and G). Expression of Opa1 decreased after treatment with H_2O_2, and the decrease was greater in the *Idh2*-siRNA–transfected cells (Figure 8, A and I). *Idh2*-siRNA transfection alone, without H_2O_2 treatment, did not affect the expression of Bax (5B7), Bax (6A7), Bcl-2, XIAP, Bcl-xL, cleaved caspase-3, or Opa1 (Figure 8, A–I). H_2O_2 treatment increased the amount of TUNEL-positive cells and this increase was greater in *Idh2*-siRNA–transfected cells than in scramble-siRNA–transfected cells (Figure 8, J and K). Total cell number was less in *Idh2*-siRNA–transfected cells than in scramble-siRNA–transfected cells (Figure 8, J and L), indicating that cell survival rate was lower in *Idh2*-siRNA–transfected cells than scramble-siRNA–transfected cells.

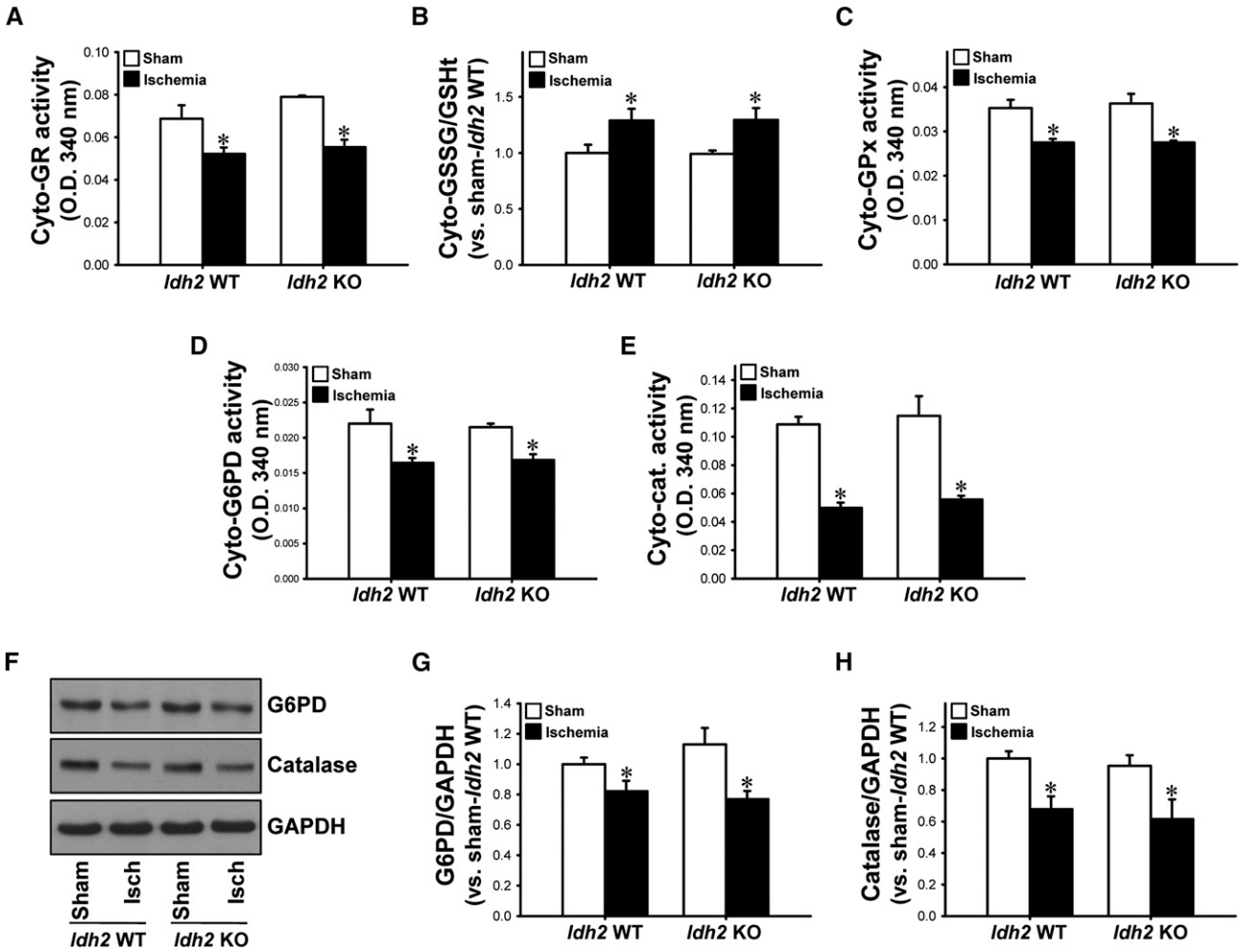

Figure 5. Expressions and activities of cytosolic GR, GPx, G6PD, catalase, and GSSG/tGSH in the cytosol of *Idh2*$^{+/+}$ and *Idh2*$^{-/-}$ mice after I/R. *Idh2*$^{+/+}$ (*Idh2* WT) and *Idh2*$^{-/-}$ (*Idh2* KO) mice were subjected to either 25 minutes of bilateral renal ischemia or sham surgery. Activities of GR (A), GPx (C), G6PD (D), catalase (E), and GSSG/tGSH (B) in the cytosol fraction were determined. (F) Kidney samples were subjected to Western blot analysis using anti-G6PD and anti-catalase antibodies. GAPDH was used as loading control. (G and H) Densities of blots were measured using ImageJ software. Results are expressed as the mean±SEM (n=6). *P<0.05 versus respective sham-operated mice. Cat, catalase; Cyto, cytosolic; Isch, ischemia; KO, knockout; WT, wild type.

Next, we determined the role of IDH2 on ATP depletion/repletion-induced hypoxic injury. *Idh2*-siRNA transfection significantly decreased IDH2 expression in the cells (Figure 8, M and N). ATP depletion/repletion decreased the expression of IDH2 in both *Idh2*-siRNA-transfected cells and scramble-siRNA–transfected cells (Figure 8, M and N). ATP depletion/repletion increased the amount of TUNEL-positive cells in both *Idh2*-siRNA–transfected cells and scramble-siRNA–transfected cells, and these increases were greater in *Idh2*-siRNA–transfected cells than in scramble-siRNA–transfected cells (Figure 8, O and P). ATP depletion/repletion reduced total cell number, and this reduction was greater in *Idh2*-siRNA–transfected cells than in scramble-siRNA–transfected cells (Figure 8, O and Q). Taken together, these results indicate that IDH2 protects kidney tubule cells against mitochondrial damage and apoptosis induced by oxidative stress and hypoxic injury.

DISCUSSION

We demonstrate, for the first time, that I/R causes disruption of IDH2, and that *Idh2* gene deletion exacerbates I/R-induced defects in the structure and function of mitochondria *via* impairment of the NADPH–GR–GSH–GPx antioxidant systems. Furthermore, *Idh2* gene deletion delays recovery from injury. This results in increased mitochondrial and cellular oxidative damage, leading to apoptosis, and structural and functional impairments of the kidneys. These findings indicate that IDH2 is important for maintaining redox balance and for protecting the kidneys from I/R insult. This suggests that IDH2 is a therapeutic target for AKI treatment, in addition to mitochondrial dysfunction-related diseases.

I/R insult disrupts the mitochondrial redox balance in kidney tissue, resulting in a shutdown of mitochondrial energy

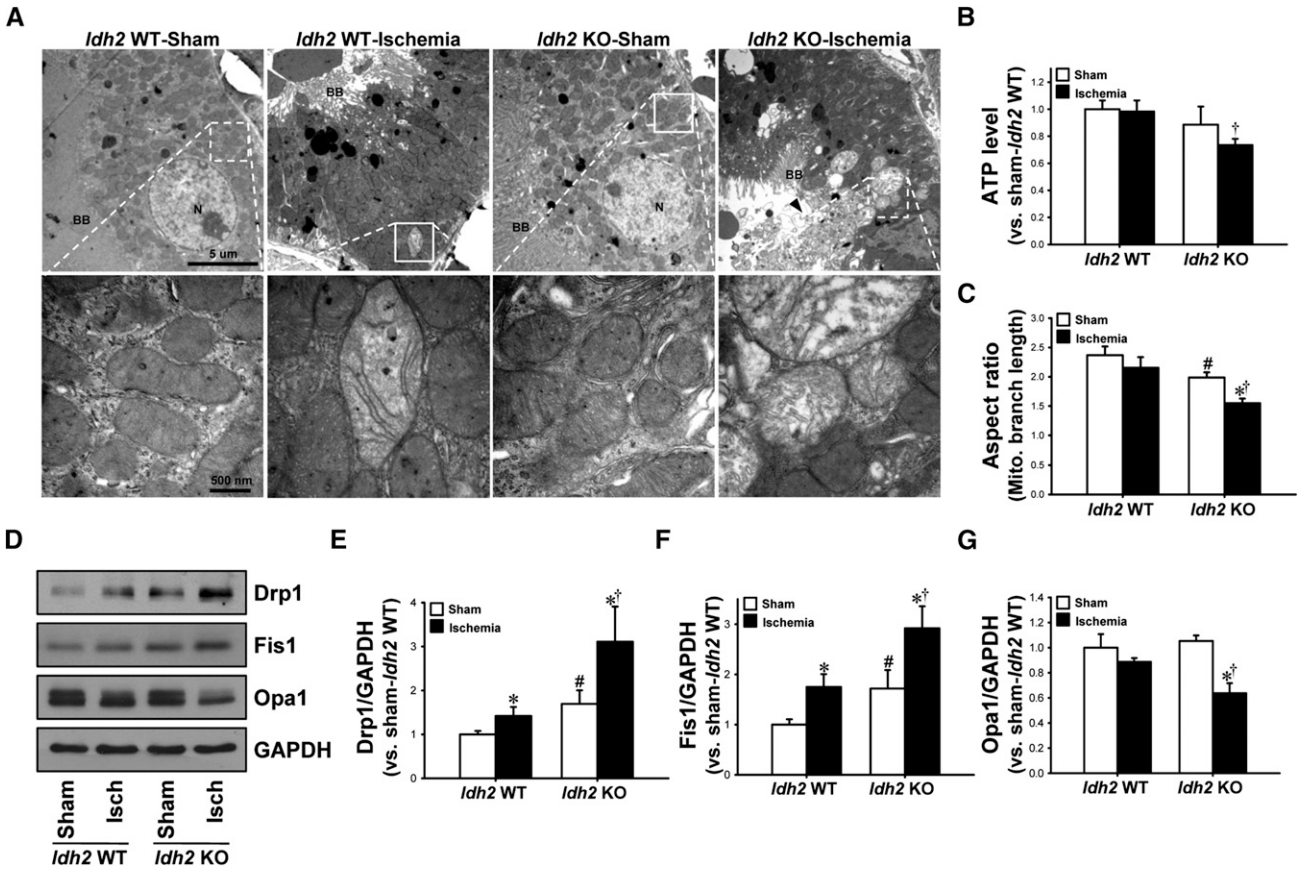

Figure 6. Mitochondrial function and structures in *Idh2*$^{+/+}$ and *Idh2*$^{-/-}$ mice after I/R injury. *Idh2*$^{+/+}$ (*Idh2* WT) and *Idh2*$^{-/-}$ (*Idh2* KO) mice were subjected to either 25 minutes of bilateral renal ischemia or sham surgery. (A) Ninety minutes after ischemia or sham surgery, mitochondrial structures were evaluated under transmission electron microscopy (TEM). Upper panels are at low magnification. Lower panels are at high magnification of the dash-lined rectangle in the upper panels and show mitochondrial structures. (B) Twenty-four hours after ischemia, ATP levels were measured as described in the Concise Methods. (C) Aspect ratio [(major axis)/(minor axis)] from TEM pictures was measured. (D) Twenty-four hours after surgery, kidneys samples were subjected to Western blot analysis using anti-Drp1, anti-Fis1, and anti-Opa1 antibodies. GAPDH was used as a loading control. (E–G) Densities of blots were measured using ImageJ software. Results are expressed as mean±SEM (n=6). *P<0.05 versus respective sham-operated mice; $^{\dagger}P$<0.05 versus ischemia-operated *Idh2* WT; $^{\#}P$<0.05 versus sham-operated *Idh2* WT. BB, Brush border; Isch, ischemia; KO, knockout; N, Nucleus; WT, wild type.

production, and in the occurrence of oxidative damage to mitochondrial and cellular proteins, lipids, and nucleic acids, which causes apoptosis, necrosis, and inflammation in the kidney.[14,15,22] In this study, *Idh2* gene deletion reduced the amount of NADPH in both sham- and I/R-operated mouse kidneys. GSSG/tGSH was elevated to a greater extent after I/R in mitochondria from *Idh2*$^{-/-}$ mice than from *Idh2*$^{+/+}$ mice, indicating that mitochondrial GSSG could not be reduced to GSH by GR because of insufficient mitochondrial NADPH in *Idh2*$^{-/-}$ mice. In addition, *Idh2* gene deletion diminished the ROS-scavenging activity of GPx in the mitochondria after I/R, accompanied by increases in H_2O_2 production, lipid peroxidation, and oxidative damage to mtDNA. In I/R-induced AKI models, Mortensen *et al.* and Liang *et al.* have reported that MnTMPyP, an MnSOD mimetic, protects kidneys from I/R-induced ROS production, inflammatory responses, and apoptosis.[15,22] Dare *et al.* reported that MitoQ, an antioxidant targeted to mitochondria, ameliorates I/R-induced oxidative stress and kidney injury.[16] We previously reported that *Idh2* gene deficiency increases ROS production and oxidative stress, leading to mitochondrial damage,[6–8] whereas *Idh2* gene induction dampens various stresses, including H_2O_2, cadmium, heat shock, high glucose, and ethanol.[6,9,23–25] Recently it has been reported that IDH2 plays an important role in maintenance of redox balance and mitochondrial homeostasis in endothelial cells.[26] Therefore, our results indicate that IDH2 serves as an important provider of NADPH in the mitochondria, and IDH2 deficiency increases the susceptibility of mitochondria to post-I/R oxidative stress.

IDH1 is expressed in the cytosol, whereas IDH2 is expressed in the mitochondria. IDH2 is $NADP^+$-dependent and IDH3, although it is located on the mitochondria, is a NAD^+-dependent enzyme.[6,21,27] In this study, we found that activity and expression of IDH1 before and 24 hours after I/R insult were less in *Idh2*$^{-/-}$ mice when compared with *Idh2*$^{+/+}$ mice. Because cytosolic oxidative stress influences mitochondrial

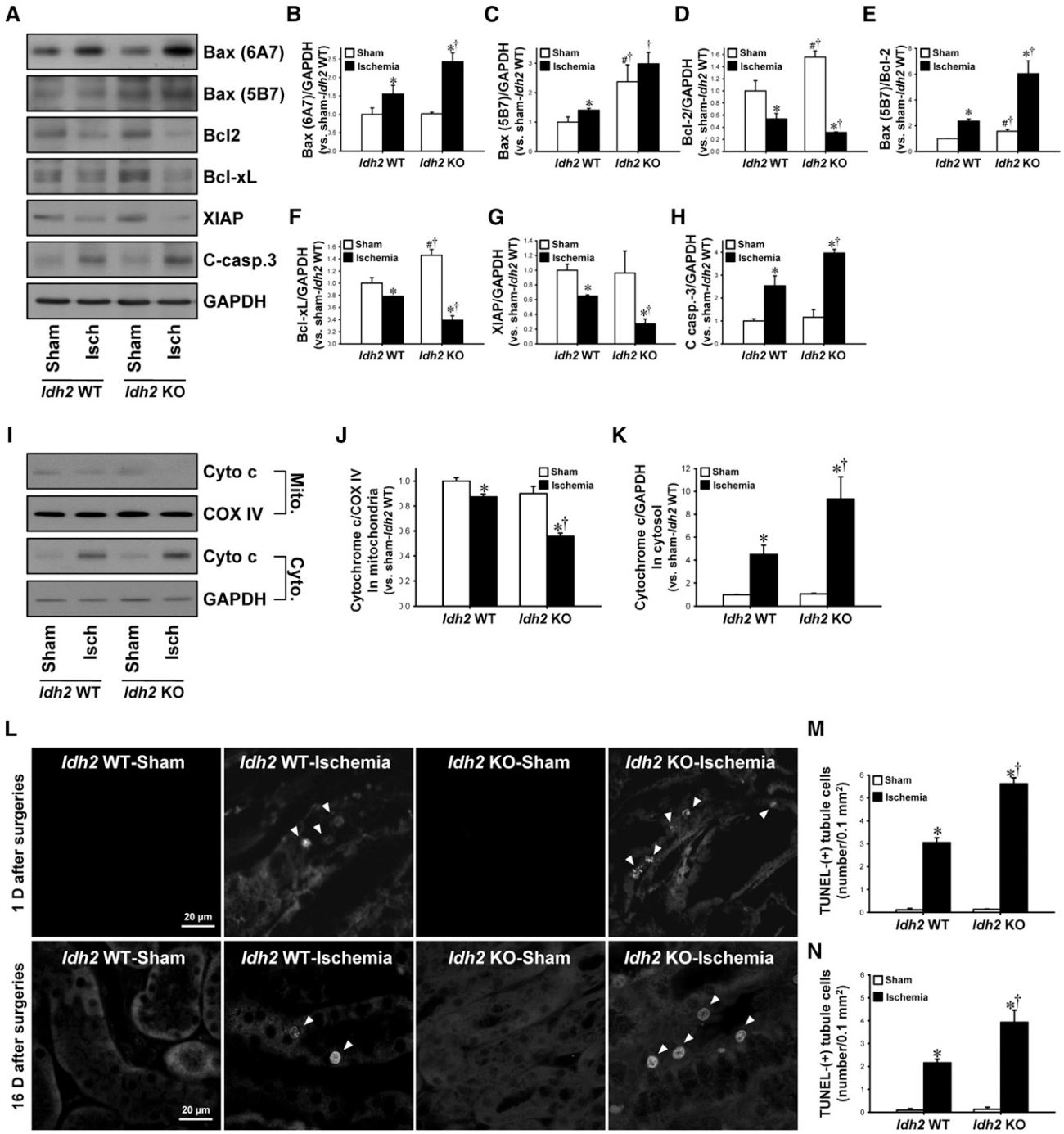

Figure 7. Apoptosis and its signal pathways in *Idh2*$^{+/+}$ and *Idh2*$^{-/-}$ mice after I/R injury. *Idh2*$^{+/+}$ (*Idh2* WT) and *Idh2* $^{-/-}$ (*Idh2* KO) mice were subjected to either 25 minutes of bilateral renal ischemia or sham surgery. Twenty-four hours after ischemia, (A) Kidney tissue samples were analyzed by Western blotting using antibodies directed against Bax (6A7), Bax (5B7), Bcl-2, Bcl-xL, XIAP, and cleaved caspase-3. GAPDH was used as a loading control. (B–H) The densities of bands were measured using ImageJ software. (I) Mitochondrial (Mito.) and cytosolic (Cyto.) fractions were subjected to Western blot analysis using anti-cytochrome *c* (Cyto c) antibody. COX IV and GAPDH were used as a loading control of mitochondrial and cytosolic fraction, respectively. (J and K) The densities of bands were measured using ImageJ software. (L) Apoptotic cells in kidney tissue were evaluated by TUNEL assay 24 hours (upper panels) and 16 days (lower panels) after surgery. Arrows indicate TUNEL-positive cells. Images were obtained from the outer stripe of outer medulla. 4′,6-diamidino-2-phenylindole was used to stain the nuclei of cells. (M and N) TUNEL-positive cells were counted (ten fields per kidney). Results are expressed as mean±SEM (n=6). *P<0.05 versus sham-operated *Idh2* WT mice; $^{\dagger}P$<0.05 versus ischemia-operated *Idh2* WT mice; $^{\#}P$<0.05 versus sham-operated *Idh2* WT. Isch, ischemia; KO, knockout; WT, wild type.

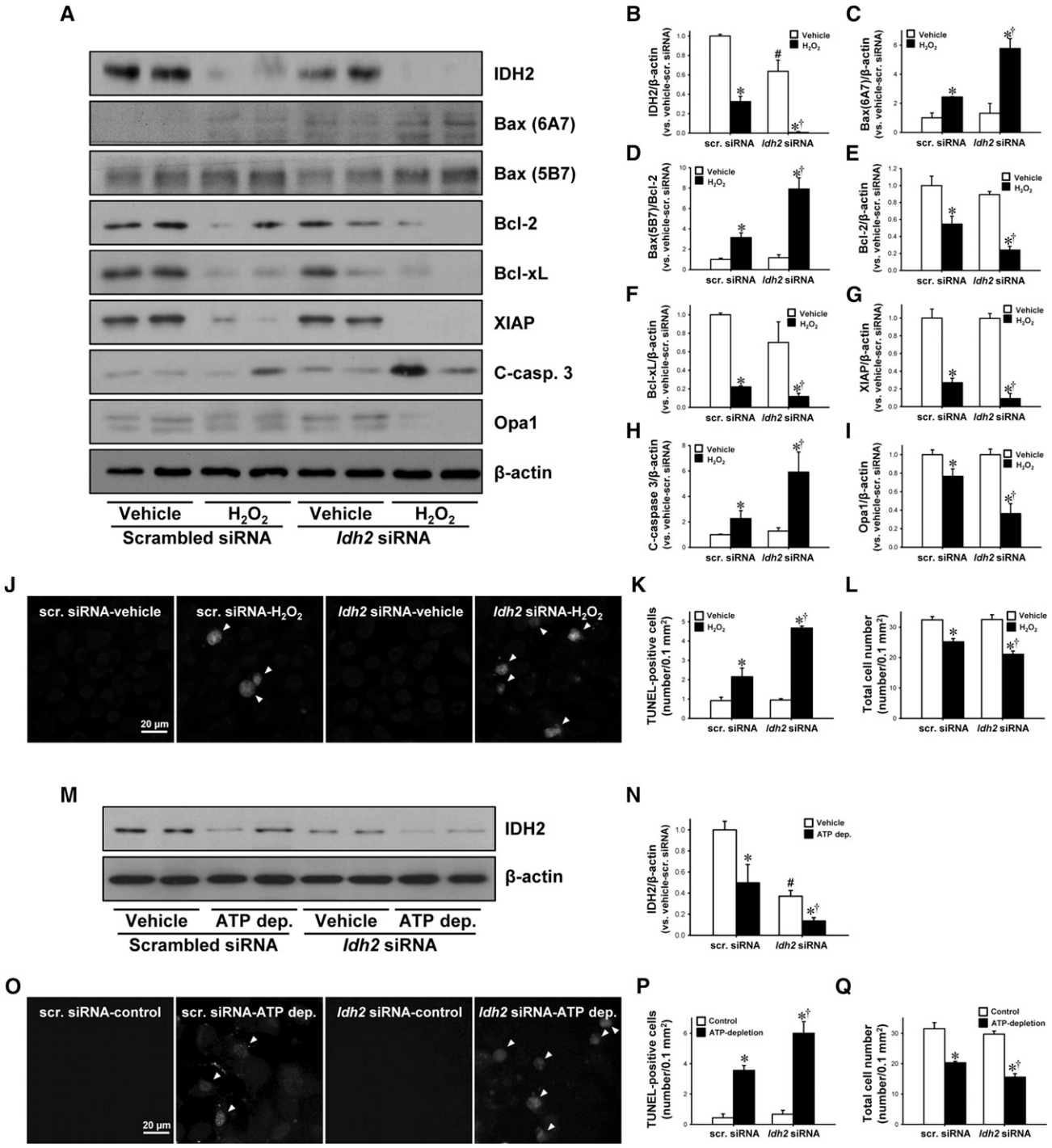

Figure 8. Effect of IDH2 downregulation on H_2O_2-induced apoptosis in cultured mProx24 cells. mProx24 cells were transfected with *Idh2*-siRNA and scrambled siRNA (Scr-siRNA). After transfection, cells were treated with 500 μM H_2O_2 for 5 hours. (A) Cell lysates were analyzed by Western blotting using antibodies directed against IDH2, Bax (6A7), Bax (5B7), Bcl-2, Bcl-xL, XIAP, cleaved caspase-3 (C-casp-3), and Opa1. β-actin was used as a loading control. (B–I) The densities of bands were measured using ImageJ software. (J) Fixed cells were subjected to TUNEL assay. Arrows indicate TUNEL-positive cells. TUNEL-positive (K) and total cell number (L) were determined. (M–Q) mProx24 cells transfected with either *Idh2*-siRNA or Scr-siRNA were incubated in Krebs–Henseleit buffer with or without sodium cyanide (5 mM) and 2-deoxyglucose (5 mM) for 60 minutes, followed by Krebs–Henseleit buffer containing 10 mM of dextrose for 40 minutes. Cells were subjected to Western blot analysis using anti-IDH2 antibody. β-actin was used as a loading control. (N) The densities of bands were measured using ImageJ software. (O) Fixed cells were subjected to TUNEL assay. Arrows indicate TUNEL-positive cells. TUNEL-positive (P) and total cell number (Q) were counted. Results are expressed as mean±SEM (n=3). *$P<0.05$ versus respective vehicle-treated siRNA; $^{\dagger}P<0.05$ versus H_2O_2-treated or ATP-depleted Scr. siRNA; $^{\#}P<0.05$ versus vehicle-treated Scr. siRNA. ATP dep., ATP depletion.

oxidative stress and *vice versa*, these decreases of IDH1 activity and expression in *Idh2*$^{-/-}$ mice may, at least in part, contribute to increases in mitochondrial damage, leading to increased susceptibility in *Idh2*$^{-/-}$ mice. It is also possible that IDH1 and IDH2 interact with each other. There is some evidence that IDH2 and IDH1 may interact or share similar expression patterns; mutations of *Idh1* and *Idh2* are frequent in some types of cancer, including leukemia, gliomas, and cartilaginous tumors.[27–30] However, 16 days post-I/R, mortality of *Idh2*$^{-/-}$ mice was almost 65%, whereas that of *Idh2*$^{+/+}$ mice was about 30% (Figure 1A). Furthermore, in this study, the expression and activity of G6PD, a major NADPH-producing enzyme in the cytosol, were not different between *Idh2*$^{-/-}$ and *Idh2*$^{+/+}$ mice after both sham and I/R operation. In addition, the activities of GPx/GR in the cytosol were not significantly different between *Idh2*$^{-/-}$ and *Idh2*$^{+/+}$ mice. These results indicate that, although IDH1 could be involved in the increased susceptibility of IDH2 to I/R injury, IDH2 plays a critical role in the kidney post-I/R injury.

In this study, I/R decreased IDH3 activity in both *Idh2*$^{-/-}$ and *Idh2*$^{+/+}$ mice. However, this decrease rate was not significantly different between *Idh2*$^{-/-}$ and *Idh2*$^{+/+}$ mice. In addition, there was no difference in IDH3 activity between sham-operated *Idh2*$^{-/-}$ and *Idh2*$^{+/+}$ mice. This suggests that, although IDH3 may be affected by I/R injury, it is not critical for the increased susceptibility to I/R injury shown in *Idh2*$^{-/-}$ mice. In previous studies, we found that the regulation of IDH2 expression (overexpression or knockdown) did not affect IDH3 activity.[6] Although we could not rule out the involvement of IDH1 and IDH3 in the increased susceptibility of *Idh2*$^{-/-}$ mice, taken together, IDH2 plays a critical role in injury and repair after I/R injury.

Mitochondria are dynamic organelles and their morphology is maintained through a balance between fission and fusion processes.[12] Under physiologic conditions, mitochondria are filamentous and elongated, whereas under stress conditions, including I/R injury, mitochondria become fragmented and degraded. Such fragmentation and degradation induces an increase in permeability of the mitochondrial outer membrane and enables the release of proapoptotic factors, such as cytochrome *c*.[12] Mitochondrial fission involves the constriction and cleavage of mitochondria by fission proteins, such as Drp1 and Fis1. Conversely, mitochondrial fusion involves the elongation of mitochondria by tethering and merging two adjacent mitochondria. Mitochondrial fusion is mediated by Mitofusin-1 and Mitofusin-2 in the outer membrane, and by Opa1 in the inner membrane.[12] Brooks *et al.* reported that mitochondrial fragmentation precedes cytochrome *c* release, apoptosis, and AKI in I/R- and cisplatin-induced models.[31] They also reported that inhibition of mitochondrial fragmentation using mdivi-1, a pharmacologic inhibitor of Drp1, ameliorates tubular cell apoptosis and AKI.[31] Xiao *et al.* reported that *Oma1* gene deficiency prevents Opa1 proteolysis, and this protects against mitochondrial fragmentation and AKI after I/R.[32] In our study, the expression of Fis1 and Drp1 was higher in *Idh2*$^{-/-}$ mice than in *Idh2*$^{+/+}$ mice. This was the case even when sham-operated *Idh2*$^{-/-}$ mice were compared with *Idh2* $^{+/+}$ mice, which had severe mitochondrial fragmentation. In addition, ATP levels 24 hours post-ischemia were significantly lower in *Idh2*$^{-/-}$ mice, but not in *Idh2*$^{+/+}$ mice, when compared with sham-operated mice. Because ATP levels decrease quickly upon ischemia and return to a normal range within a few hours after reperfusion,[33,34] the lowered ATP levels in *Idh2*$^{-/-}$ mice may reflect the delayed recovery of the kidneys from I/R injury, suggesting that IDH2 has a critical role in the restoration of mitochondrial function.

It is known that the mitochondria are central players in apoptosis. When electron transport and energy metabolism become impaired, mitochondria can trigger apoptosis by releasing cytochrome *c*, activating caspases, and altering the cellular redox potential *via* ROS production.[11,12] In this study, I/R led to increases in cytochrome *c* release, caspase-3 cleavage, and TUNEL-positive apoptotic cells, and these increases were greater in *Idh2*$^{-/-}$ mice than in *Idh2*$^{+/+}$ mice. In addition, *Idh2* gene deletion enhanced the post-I/R increase in the ratio of Bax-to-Bcl-2. This indicates that *Idh2* gene deletion exacerbates apoptosis in mouse kidneys. Further, it was demonstrated that IDH2 downregulation by *Idh2*-siRNA accelerated apoptosis after treatment with H_2O_2 and ATP depletion. This suggests that the mitochondrial dysfunction because of IDH2 downregulation can activate the apoptosis signaling pathway.

In conclusion, this study demonstrates that IDH2 is an important antioxidant enzyme that protects against mitochondrial damage, oxidative stress, apoptosis, and necrosis *via* the production of NADPH, which is an essential cofactor for the GSH–GPx antioxidant system.

CONCISE METHODS

Animal Preparation

All experiments were conducted using 8- to 10-week-old *Idh2* knockout (*Idh2*$^{-/-}$) and wild-type (*Idh2*$^{+/+}$) male mice weighing 22–24 g.[8] The generation and characterization of *Idh2*$^{-/-}$ mice has been described previously.[8] This study was conducted in accordance with the guidelines of the Institutional Animal Care and Use Committee of Kyungpook National University, Republic of Korea, and the Guide for the Care and Use of Laboratory Animals, published by the US National Institutes of Health (Publication No. 85–23, revised 2011). The mice were provided free access to water and standard chow. The mice were anesthetized by intraperitoneal injection of pentobarbital sodium before surgery (50 mg/kg body wt; Sigma-Aldrich, St. Louis, MO). To induce ischemia, kidneys were exposed *via* flank incisions, and the renal pedicles were clamped completely for 25 minutes using microaneurysm clamps while mice were under anesthetic. The same procedure, except for the clamping of the renal pedicle, was used during the sham operation. Body temperature was maintained at 36.5°C–37°C throughout all surgical procedures by using a temperature-controlled heating device (FHC, Bowdoinham, ME). After surgery, PCr and BUN concentrations were determined to evaluate renal function by using a Vitros 250 Chemistry Analyzer (Johnson & Johnson, Rochester, NY).

The kidneys were excised 1 day postsurgery and were either snap-frozen in liquid nitrogen for Western blot analysis, or perfusion-fixed in PLP (4% paraformaldehyde, 75 mM L-lysine, and 10 mM sodium periodate; Sigma-Aldrich) for histologic studies.

Histology

Kidneys were perfusion-fixed with PLP and paraffin sections were stained with periodic acid–Schiff stain, according to a standard protocol. To determine morphologic damage to tubular cells, kidney damage in a kidney section stained with periodic acid–Schiff was scored at ten fields in the outer medulla per kidney, as described previously.[35]

Picro-Sirius Red Staining

Paraffin-embedded kidney tissue sections were stained with picro-sirius red (PSR), according to the standard protocol. Dewaxed kidney tissue sections were exposed to PSR stain for 1 hour, and then washed twice with acidified water (0.5% glacial acetic acid). Sections were then serially dehydrated in different alcohol concentrations. Photomicrographs (400× magnification) were obtained randomly from the outer medullary region using a Leica microscope (DM2500; Leica Microsystems, Buffalo Grove, IL). Regions of collagen deposition in PSR-stained kidney sections were measured using an image analysis program (i-solution; Image & Microscope Technology Inc., Daejeon, Republic of Korea).

Western Blot Analysis

Western blotting was performed as described previously.[36] Western blotting was performed using antibodies directed against mitochondrial $NADP^+$-dependent IDH2,[24] cytosolic $NADP^+$-dependent IDH1,[37] MnSOD (Calbiochem, San Diego, CA), copper-zinc superoxide dismutase (CuZnSOD; Chemicon, Temecula, CA), Opa1 (BD Biosciences, San Jose, CA), Drp1 (Cell Signaling Technology, Danvers, MA), Fis1 (Sigma-Aldrich), Bax (5B7) (EMD Millipore, Billerica, MA), Bax (6A7) (Santa Cruz Biotechnology, Santa Cruz, CA), Bcl-2 (EMD Millipore), XIAP (AnaSpec, San Jose, CA), Bcl-xL (BD Biosciences), cleaved caspase-3 (Cell Signaling Technology), 4-HNE (Abcam, Inc., Cambridge, MA), G6PD (Cell Signaling Technology), catalase (Fitzgerald, Concord, MA), Ly6G (eBioscience, San Diego, CA), cytochrome *c* (BD Biosciences), COX-IV (Abcam, Inc.), β-actin (Sigma-Aldrich), and GAPDH (Novus Biologicals, Littleton, CO).

Immunofluorescence Staining

Immunofluorescence staining of IDH2 was performed as previously described.[38] Immunofluorescence staining of the proximal tubules and the descending limb of the loop of Henle was performed using antibodies directed against Aquaporin 1 (AQP1; Alomone Labs, Jerusalem, Israel). Staining of the distal tubules was performed using antibodies directed against Na^+/Ca^{2+} exchanger 1 (NCX1; Thermo Fischer Scientific, Vernon Hills, IL), as described previously.[19] Sections were viewed under a Leica microscope (DM2500).

Immunohistochemical Staining

Immunohistochemical staining was performed using anti-NADPH (1:100; Biorbyt, Cambridge, UK), 8-OHdG (Abcam, Inc.), and anti-F4/80 (Serotec, Oxford, UK) antibodies, as described previously.[19] The 8-OHDG antibody binds to DNA damaged by oxidation in mitochondria and nuclei.[20] Sections were viewed under a Leica microscope (DM2500). Photomicrographs were obtained randomly from the outer medullary region. F4/80– and 8-OHdG–positive cells were counted and the intensity of 8-OHdG stains were measured under 400× magnification using an image analysis program (i-solution).

Measurement of H_2O_2 and Lipid Peroxidation in the Kidney

H_2O_2 levels in the kidney tissue were measured using xylenol orange, a dye sensitive to ferric ions, as described previously.[38] To determine the extent of lipid peroxidation, thiobarbituric acid-reactive substances (Sigma-Aldrich) were used as described previously.[39]

Preparation of Cytosolic and Mitochondrial Fractions

Cytosolic and mitochondrial fractions were prepared as described previously.[40] Briefly, frozen kidney tissue was homogenized in sucrose buffer (0.2 M sucrose, 1 mM EGTA, 10 mM HEPES, pH 7.4; Sigma-Aldrich) on ice, three times using a Teflon Homogenizer (Daihan Scientific, Seoul, Korea) at 1600 rpm. The homogenate was centrifuged at 600 × *g* for 10 minutes, and then the supernatant was centrifuged at 7000 × *g* for 10 minutes. The supernatant comprised the cytosolic fraction, and it was centrifuged again at 7000 × *g* for 10 minutes, to purify the cytosolic fraction. The mitochondrial pellet was washed twice with sucrose buffer and was centrifuged again at 7000 × *g* for 10 minutes. The pellet was suspended in PBS containing 0.1% Triton X-100, disrupted twice with a sonicator (4710 series; Cole-Palmer, Chicago, IL) at 40% of the maximum setting for 10 seconds, and centrifuged at 15,000 × *g* for 30 minutes. The supernatant comprised the mitochondrial fraction, and it was used to measure the activity of enzymes. Equal amounts of fractionated proteins were separated by SDS-PAGE, transferred to a PVDF membrane, and then stained with Ponceau S reagent. Effective isolation of those fractions was confirmed by Western blot analysis, using antibodies against IDH1, CuZnSOD, and GAPDH for the cytosolic fraction, and against IDH2 and MnSOD for the mitochondrial fraction (Figure 2G).

Measurement of GSSG/tGSH in the Kidney

GSSG/tGSH was measured using an enzymatic recycling method, as described previously.[41,42] Given that GSH and related thiols are sensitive to oxidation and degradation during sampling and analysis, samples were harvested quickly in liquid nitrogen, stored at −70°C until use, and analyzed rapidly. The total amount of glutathione was determined by the formation of 5-thio-2-nitrobenzoic acid (TBA) from 5,5′-dithiobis(2-nitrobenzoic acid), as described by Akerboom and Sies.[41] GSSG was measured by the removal of TBA produced by the reaction of glutathione and 5,5′-dithiobis(2-nitrobenzoic acid) upon the addition of 2-vinylpyridine, which inhibits the formation of TBA by GSH.[42] Total GSH and GSSG levels were defined as the change in optical density at 412 nm over 1 minute at 37°C.

Measurement of ATP Levels and the Activity of IDH1 and IDH2

The activity of IDH1, IDH2, G6PD, and catalase was measured as described previously.[43] The levels of ATP were measured using an

ATP Colorimetric/Fluorometric Assay Kit according to the manufacturer's instructions (Abcam, Inc.).

mProx24 Cell Culture and IDH2 Knockdown

mProx24 cells[44] were cultured in DMEM with 10% FBS (Mediatech Inc., Manassas, VA) and 100 μl/ml of streptomycin/penicillin (WelGENE Inc., Daegu, Korea). siRNA directed against *Idh2*, and an RNA-interference negative control, were provided by ST Pharm (Seoul, Korea). Once the mProx24 cells reached 60%–70% confluency, they were transfected with siRNAs (200 pmol/μl) using Lipofectamine 2000 (Thermo Fisher Scientific) for 48 hours, according to the manufacturer's instructions. The mProx24 cells transfected with siRNAs were treated with 500 μM H_2O_2 for 5 hours, and harvested or fixed to analyze for apoptosis. To induce ATP depletion/repletion, cells were incubated in a Krebs–Henseleit buffer (115 mM NaCl, 3.6 mM KCl, 1.3 mM KH_2PO_4, 25 mM $NaHCO_3$, 1 mM $CaCl_2$, 1 mM $MgCl_2$; pH 7.4) with or without sodium cyanide (5 mM) and 2-deoxyglucose (5 mM) for 60 minutes, washed with Krebs–Henseleit buffer, and then incubated in Krebs–Henseleit buffer containing 10 mM of dextrose for 40 minutes.

TUNEL Assay

TUNEL assay was performed using an *in situ* cell death detection kit (Roche Diagnostics, Indianapolis, IN) according to the manufacturer's instructions. Briefly, 4-μm kidney sections were deparaffinized and rehydrated. Then, the sections were incubated with TUNEL reagent mixture for 30 minutes at room temperature, and washed with PBS three times, for 5 minutes each time. 4′,6-diamidino-2-phenylindole was used to stain nuclei. Images were obtained from the outer stripe of the outer medulla, under a Leica DM2500 microscope. TUNEL-positive cells were counted at ten fields per kidney.

Transmission Electron Microscopy

Ninety minutes after sham or ischemia-inducing surgery, kidneys were perfusion-fixed with 2.5% glutaraldehyde *via* the abdominal aorta, then stored overnight in the fixative at 4°C. Samples were cut into 1 mm^3, washed in 0.1 M phosphate buffer, and then postfixed in aqueous 2% osmium tetroxide for 90 minutes. After three washes with 0.1 M phosphate buffer, the samples were dehydrated through a graded series of 50%–100% ethanol, 100% propylene oxide, and then infiltrated in 1:1, 1:2, and 1:3 mixtures of propylene oxide: *Epon* Resin 828 (Polysciences Inc., Warrington, PA) for 1 hour, respectively. After samples had been incubated in 100% *Epon* Resin 828 over 8 hours, samples were then embedded in molds and cured at 35°C and 45°C for 12 hours, followed by additional hardening at 60°C for 2 days. Ultrathin (60 nm) sections were double-stained with 2% uranyl acetate and 1% lead citrate. Sections were visualized using a transmission electron microscope (H-7000; Hitachi, Yokohama, Japan) at 75 kV. Electron micrographs of mitochondria were captured from proximal tubule cells in the outer stripe of outer medulla. The mitochondrial aspect ratio [(major axis)/(minor axis)] was computed using 30 mitochondria per cell.

Statistical Analyses

Results are expressed as mean±SEM. Statistical differences among groups were calculated using paired *t* tests and one-way ANOVA. Differences were regarded as statistically significant when they had *P* values <0.05.

ACKNOWLEDGMENTS

This study was supported by grants from the National Research Foundation of Korea, funded by the Korean government (grant numbers: NRF-2014R1A2A11049549 and NRF-2015R1A2A1A15052400 to K.M.P., and NRF-2015R1A41042271 to J.-W.P.).

DISCLOSURES

None.

REFERENCES

1. Reitman ZJ, Yan H: Isocitrate dehydrogenase 1 and 2 mutations in cancer: alterations at a crossroads of cellular metabolism. *J Natl Cancer Inst* 102: 932–941, 2010
2. Nakamura H: Thioredoxin and its related molecules: update 2005. *Antioxid Redox Signal* 7: 823–828, 2005
3. Minard KI, McAlister-Henn L: Dependence of peroxisomal beta-oxidation on cytosolic sources of NADPH. *J Biol Chem* 274: 3402–3406, 1999
4. Kim J, Kim KY, Jang HS, Yoshida T, Tsuchiya K, Nitta K, Park JW, Bonventre JV, Park KM: Role of cytosolic NADP+-dependent isocitrate dehydrogenase in ischemia-reperfusion injury in mouse kidney. *Am J Physiol Renal Physiol* 296: F622–F633, 2009
5. Kakkar P, Singh BK: Mitochondria: a hub of redox activities and cellular distress control. *Mol Cell Biochem* 305: 235–253, 2007
6. Jo SH, Son MK, Koh HJ, Lee SM, Song IH, Kim YO, Lee YS, Jeong KS, Kim WB, Park JW, Song BJ, Huh TL: Control of mitochondrial redox balance and cellular defense against oxidative damage by mitochondrial NADP+-dependent isocitrate dehydrogenase. *J Biol Chem* 276: 16168–16176, 2001
7. Ku HJ, Park JW: Downregulation of IDH2 exacerbates HO-mediated cell death and hypertrophy [published online ahead of print February 15, 2016]. Redox Rep doi:10.1080/13510002.2015.1135581
8. Kim S, Kim SY, Ku HJ, Jeon YH, Lee HW, Lee J, Kwon TK, Park KM, Park JW: Suppression of tumorigenesis in mitochondrial NADP(+)-dependent isocitrate dehydrogenase knock-out mice. *Biochim Biophys Acta* 1842: 135–143, 2014
9. Yang ES, Park JW: Regulation of ethanol-induced toxicity by mitochondrial NADP(+)-dependent isocitrate dehydrogenase. *Biochimie* 91: 1020–1028, 2009
10. Bonventre JV: Mechanisms of ischemic acute renal failure. *Kidney Int* 43: 1160–1178, 1993
11. Tábara LC, Poveda J, Martin-Cleary C, Selgas R, Ortiz A, Sanchez-Niño MD: Mitochondria-targeted therapies for acute kidney injury. *Expert Rev Mol Med* 16: e13, 2014
12. Stallons LJ, Funk JA, Schnellmann RG: Mitochondrial homeostasis in acute organ failure. *Curr Pathobiol Rep* 1: 2013
13. Cappellini MD, Fiorelli G: Glucose-6-phosphate dehydrogenase deficiency. *Lancet* 371: 64–74, 2008
14. Chen YR, Zweier JL: Cardiac mitochondria and reactive oxygen species generation. *Circ Res* 114: 524–537, 2014
15. Mortensen J, Shames B, Johnson CP, Nilakantan V: MnTMPyP, a superoxide dismutase/catalase mimetic, decreases inflammatory indices in ischemic acute kidney injury. *Inflamm Res* 60: 299–307, 2011
16. Dare AJ, Bolton EA, Pettigrew GJ, Bradley JA, Saeb-Parsy K, Murphy MP: Protection against renal ischemia-reperfusion injury in vivo by the mitochondria targeted antioxidant MitoQ. *Redox Biol* 5: 163–168, 2015

17. Ng CF, Schafer FQ, Buettner GR, Rodgers VG: The rate of cellular hydrogen peroxide removal shows dependency on GSH: mathematical insight into in vivo H2O2 and GPx concentrations. *Free Radic Res* 41: 1201–1211, 2007
18. Swierczynski J, Zelewski M, Zołnierowicz S, Klimek J, Marszałek J, Zelewski L: Isolation, properties and role in progesterone biosynthesis of cytosolic malic enzyme from human term placenta. *Placenta* 8: 175–184, 1987
19. Kim J, Seok YM, Jung KJ, Park KM: Reactive oxygen species/oxidative stress contributes to progression of kidney fibrosis following transient ischemic injury in mice. *Am J Physiol Renal Physiol* 297: F461–F470, 2009
20. Valavanidis A, Vlachogianni T, Fiotakis C: 8-hydroxy-2′ -deoxyguanosine (8-OHdG): A critical biomarker of oxidative stress and carcinogenesis. *J Environ Sci Health C Environ Carcinog Ecotoxicol Rev* 27: 120–139, 2009
21. Winkler BS, DeSantis N, Solomon F: Multiple NADPH-producing pathways control glutathione (GSH) content in retina. *Exp Eye Res* 43: 829–847, 1986
22. Liang HL, Hilton G, Mortensen J, Regner K, Johnson CP, Nilakantan V: MnTMPyP, a cell-permeant SOD mimetic, reduces oxidative stress and apoptosis following renal ischemia-reperfusion. *Am J Physiol Renal Physiol* 296: F266–F276, 2009
23. Kil IS, Shin SW, Yeo HS, Lee YS, Park JW: Mitochondrial NADP+-dependent isocitrate dehydrogenase protects cadmium-induced apoptosis. *Mol Pharmacol* 70: 1053–1061, 2006
24. Shin AH, Kil IS, Yang ES, Huh TL, Yang CH, Park JW: Regulation of high glucose-induced apoptosis by mitochondrial NADP+-dependent isocitrate dehydrogenase. *Biochem Biophys Res Commun* 325: 32–38, 2004
25. Kim HJ, Kang BS, Park JW: Cellular defense against heat shock-induced oxidative damage by mitochondrial NADP+ -dependent isocitrate dehydrogenase. *Free Radic Res* 39: 441–448, 2005
26. Park JB, Nagar H, Choi S, Jung SB, Kim HW, Kang SK, Lee JW, Lee JH, Park JW, Irani K, Jeon BH, Song HJ, Kim CS: IDH2 deficiency impairs mitochondrial function in endothelial cells and endothelium-dependent vasomotor function. *Free Radic Biol Med* 94: 36–46, 2016
27. Amary MF, Bacsi K, Maggiani F, Damato S, Halai D, Berisha F, Pollock R, O'Donnell P, Grigoriadis A, Diss T, Eskandarpour M, Presneau N, Hogendoorn PC, Futreal A, Tirabosco R, Flanagan AM: IDH1 and IDH2 mutations are frequent events in central chondrosarcoma and central and periosteal chondromas but not in other mesenchymal tumours. *J Pathol* 224: 334–343, 2011
28. Gravendeel LA, Kloosterhof NK, Bralten LB, van Marion R, Dubbink HJ, Dinjens W, Bleeker FE, Hoogenraad CC, Michiels E, Kros JM, van den Bent M, Smitt PA, French PJ: Segregation of non-p.R132H mutations in IDH1 in distinct molecular subtypes of glioma. *Hum Mutat* 31: E1186–E1199, 2010
29. Mardis ER, Ding L, Dooling DJ, Larson DE, McLellan MD, Chen K, Koboldt DC, Fulton RS, Delehaunty KD, McGrath SD, Fulton LA, Locke DP, Magrini VJ, Abbott RM, Vickery TL, Reed JS, Robinson JS, Wylie T, Smith SM, Carmichael L, Eldred JM, Harris CC, Walker J, Peck JB, Du F, Dukes AF, Sanderson GE, Brummett AM, Clark E, McMichael JF, Meyer RJ, Schindler JK, Pohl CS, Wallis JW, Shi X, Lin L, Schmidt H, Tang Y, Haipek C, Wiechert ME, Ivy JV, Kalicki J, Elliott G, Ries RE, Payton JE, Westervelt P, Tomasson MH, Watson MA, Baty J, Heath S, Shannon WD, Nagarajan R, Link DC, Walter MJ, Graubert TA, DiPersio JF, Wilson RK, Ley TJ: Recurring mutations found by sequencing an acute myeloid leukemia genome. *N Engl J Med* 361: 1058–1066, 2009
30. Marcucci G, Haferlach T, Döhner H: Molecular genetics of adult acute myeloid leukemia: prognostic and therapeutic implications. *J Clin Oncol* 29: 475–486, 2011
31. Brooks C, Wei Q, Cho SG, Dong Z: Regulation of mitochondrial dynamics in acute kidney injury in cell culture and rodent models. *J Clin Invest* 119: 1275–1285, 2009
32. Xiao X, Hu Y, Quirós PM, Wei Q, López-Otín C, Dong Z: OMA1 mediates OPA1 proteolysis and mitochondrial fragmentation in experimental models of ischemic kidney injury. *Am J Physiol Renal Physiol* 306: F1318–F1326, 2014
33. Kim J, Devalaraja-Narashimha K, Padanilam BJ: TIGAR regulates glycolysis in ischemic kidney proximal tubules. *Am J Physiol Renal Physiol* 308: F298–F308, 2015
34. Vogt MT, Farber E: On the molecular pathology of ischemic renal cell death. Reversible and irreversible cellular and mitochondrial metabolic alterations. *Am J Pathol* 53: 1–26, 1968
35. Jang HS, Kim J, Park YK, Park KM: Infiltrated macrophages contribute to recovery after ischemic injury but not to ischemic preconditioning in kidneys. *Transplantation* 85: 447–455, 2008
36. Jang HS, Kim J, Kim KY, Kim JI, Cho MH, Park KM: Previous ischemia and reperfusion injury results in resistance of the kidney against subsequent ischemia and reperfusion insult in mice; a role for the Akt signal pathway. *Nephrol Dial Transplant* 27: 3762–3770, 2012
37. Lee SM, Koh HJ, Park DC, Song BJ, Huh TL, Park JW: Cytosolic NADP (+)-dependent isocitrate dehydrogenase status modulates oxidative damage to cells. *Free Radic Biol Med* 32: 1185–1196, 2002
38. Han SJ, Kim JI, Park JW, Park KM: Hydrogen sulfide accelerates the recovery of kidney tubules after renal ischemia/reperfusion injury. *Nephrol Dial Transplant* 30: 1497–1506, 2015
39. Buege JA, Aust SD: Microsomal lipid peroxidation. *Methods Enzymol* 52: 302–310, 1978
40. Frezza C, Cipolat S, Scorrano L: Organelle isolation: functional mitochondria from mouse liver, muscle and cultured fibroblasts. *Nat Protoc* 2: 287–295, 2007
41. Akerboom TP, Sies H: Assay of glutathione, glutathione disulfide, and glutathione mixed disulfides in biological samples. *Methods Enzymol* 77: 373–382, 1981
42. Anderson ME: Determination of glutathione and glutathione disulfide in biological samples. *Methods Enzymol* 113: 548–555, 1985
43. Kim J, Kim JI, Jang HS, Park JW, Park KM: Protective role of cytosolic NADP(+)-dependent isocitrate dehydrogenase, IDH1, in ischemic preconditioned kidney in mice. *Free Radic Res* 45: 759–766, 2011
44. Takaya K, Koya D, Isono M, Sugimoto T, Sugaya T, Kashiwagi A, Haneda M: Involvement of ERK pathway in albumin-induced MCP-1 expression in mouse proximal tubular cells. *Am J Physiol Renal Physiol* 284: F1037–F1045, 2003